Journal of Polymers and the Environment (2020) 28:1190–1203
https://doi.org/10.1007/s10924-020-01675-1

ORIGINAL PAPER

Effects of Various Methods of Chemical Modification of Lignocellulose Hazelnut Shell Waste on a Newly Synthesized Bio-based Epoxy Composite

Suheyla Kocaman[1] · **Gulnare Ahmetli**[1]

Published online: 12 February 2020

Abstract
In this study, a novel bio-based epoxy resin (ESA) with curable double bonds was synthesized by esterification reaction between sebacic acid (SAc) and epichlorohydrin (ECH). Its chemical structure was confirmed by FT-IR and ^{1}H NMR. Untreated, alkali treated, acrylic acid (AcA)- and acetic anhydride (AA) modified hazelnut shell waste (HSh) were used as inexpensive reinforcing materials in the ESA matrix system. The composites were prepared with HSh in varied per cent values (10–50 wt%) using the casting technique. The effects of chemical modification and amount of reinforcement materials on the properties of the composites were investigated. The composites were characterized using mechanical tests, as well as SEM, XRD, TGA, and contact angle measurement. The morphological results indicate an improvement in adhesion between the HSh fillers and ESA matrix upon chemical treatments. The modified HShs reinforced composites showed an increase of 7.7–46.2% in elongation at break when compared to the untreated HSh reinforced composite at more appropriate 20 wt% of filler. Also, tensile strengths of all chemically modified HSh composites are higher than that obtained with neat ESA and untreated HSh composites. It was observed that 20 wt% AA-modified HSh composite exhibited higher tensile strength (66 MPa) and elasticity modulus E (6.72 GPa) values. The TGA analysis showed that the HShs can significantly improve the thermal stability of neat ESA. Vicat softening temperature (VST) of composites was obtained higher than epoxy matrix. Additionally, all composites exhibited hydrophobic surfaces. The incorporation of HSh fillers reduces the wetting and hydrophilicity of synthesized epoxy resin.

Keywords Bioepoxy resin · Hazelnut shell waste · Chemical modification · Composite

Introduction

Presently, more than 75% of epoxy resins are of the bisphenol-A type, which are synthesized from petrochemical-based monomers. Investigations are underway for the synthesis of bio-based epoxy resins that are biodegradable and exhibit low toxicity [1]. Several methods have been established for the production of bio-based epoxy materials: use of bio-based monomers such as glycerol-derived epichlorohydrin (ECH) for resin synthesis, use of bio-based curing agents such as cardanol-based novolac, and epoxidation of vegetable oils for blending [2]. The bio-based content of the epoxy matrix may be raised by replacing of bisphenol-A type epoxy resin with epoxidized vegetable oils [3–5]. Park et al. [6] and Thulasiraman et al. [7] synthesized epoxidized soybean oil and epoxidized castor oil by the reaction of soybean and castor oil, respectively, with glacial acetic acid/H_2O_2. In addition, bio-based epoxy resins can be synthesized from the reactions between ECH and monomers derived from natural compounds such as tannins, catechin and lignin. Natural polyacids such as lactic acid, succinic acid, itaconic acid, and levulinic acid can be extracted from starch and sugar, and facilitate a novel method of synthesis of epoxy resins [8]. In this context, a novel itaconic acid-based epoxy resin with curable double bonds was synthesized by esterification between the acid and ECH [9].

Apart from bio-based epoxy resins, eco-friendly composite materials can be produced from natural wastes. A large quantity of plant wastes such as vegetable fibers (cellulose,

✉ Gulnare Ahmetli
gahmetli@ktun.edu.tr

[1] Department of Chemical Engineering, Faculty of Engineering and Natural Sciences, Konya Technical University, Campus, 42022 Konya, Turkey

jute, abaca, etc.) or lignocellulosic particles (hemp hurd, nutshell, coconut shell, etc.) can be used as bio-fillers in epoxy composite materials [10–13]. They not only improve the bio-content of the materials but also reduce their cost of production. In several studies, the biodegradable matrix and natural fillers were combined to create new classes of biodegradable composites with improved mechanical and thermal properties. Hazelnut shell (HSh) is a significant waste generated by the hazelnut industry that can be found in countries of Mediterranean Sea region. It grows mainly in Turkey, Spain, and Italy. However, Turkey is responsible for the highest amount of hazelnut production globally (ca. 75%) which corresponds to around 650,000 tons/year. Hence, this high production amount comes with a price by causing large quantity of hazelnut shell as waste. These waste hazelnut shells are mainly utilized as a fuel and biomass [14]. Without considering the high phenolic content of the shell, there are limited studies on its use in industrial applications, especially in the preparation of composites. The most preferred biomatrix in these composites is poly(lactic acid) (PLA) [15, 16]. The results obtained by Balart et al. [17, 18] indicate that hazelnut shell can optimally be used as reinforcing filler in fully biodegradable composites with PLA matrix. Hazelnut shell in combination with jute fiber has found application as natural and biodegradable fillers in non-asbestos organic non-metallic friction composites in which phenolic resin was used as a binder [19]. Flexible polyurethane foams were synthesized with the addition of environment-friendly fillers such as walnut shells and HShs for enhanced ecological potential and improvement in some of their properties [20]. Also several studies on another thermoplastic and thermoset polymers, such as polypropylene, urea–formaldehyde, epoxy resin filled with HSh have been published in the literature [21–24].

In the present study, we synthesized a new bio-based epoxy resin from the reaction of naturally occurring dicarboxylic sebacic acid (SAc) with ECH and used it as a matrix in the preparation of composites. The HShs were then chemically modified with NaOH, AcA, and acetic anhydride (AA), and the effects of the different modification methods on the mechanical, thermal, and water wettability properties of the composites were investigated.

Experimental

Materials

The hardener aromatic *m*-xylene diamine (MXDA) and epoxy embedding medium accelerator 2,4,6-tris(dimethylaminomethyl)phenol were purchased from Sigma-Aldrich. The chemicals for the synthesis of the new epoxy resin—sebacic acid (SAc), epichlorohydrin (ECH), and tetrabutylammonium bromide (TBAB)–were also procured from Sigma-Aldrich. The Turkish HSh used in this research was obtained from a local market, ground in an IKA A11 basic mill and sieved.

Synthesis of Bio-based Epoxy Resin (ESA)

A novel bio-based epoxy resin was synthesized by esterification [9] of 16.67 g of SAc (in a 3-necked round-bottomed flask with a magnetic stirrer, a thermometer, and a reflux condenser) with 100 mL of ECH in the presence of 0.5 g of TBAB by stirring and heating at 105 ºC for 0.5 h under N_2 flow. The temperature was then reduced to 50 ºC, and 50% NaOH solution was added dropwise to the reaction mixture, which was then heated for 3 h. At the end of the reaction, the mixture obtained was cooled to room temperature and washed in a separation funnel. Excess ECH was removed on a rotary evaporator. The synthesis reaction scheme of the SAc-based epoxy resin (ESA) is shown in Fig. 1.

Chemical Treatment of HSh

Alkali Treatment

Alkali concentration above 6% may cause significant reduction in lignocellulose fiber strength [25]. Therefore, for chemical treatment, HSh was shaken in 5% NaOH (pH 14.2) solution for 72 h at room temperature. It was then washed, dried, and ground into powder.

Acrylic Acid Treatment

Sodium hydroxide-treated HSh was treated in 1% acrylic acid (AcA) solution at 50 ºC for 1 h, then washed with distilled water and dried in an oven for 72 h at 70 ºC.

Acetylation

The alkali-treated HSh was soaked in glacial acetic acid for 1 h. The shells were separated by decanting and soaked in AA containing 2 drops of concentrated H_2SO_4 for 2 min. The shells were then withdrawn, washed well with water and dried in an oven at 80 °C.

Composite Preparation

The ground HSh-based fillers (particle size < 106 µm, obtained using a 230-mesh sieve) were mixed in various quantities (10–50 wt%) with the epoxy matrix by mechanical stirring and the mixture was subjected to ultrasound treatment for 1 h at 60 ºC. The curing agent (30 wt%) and epoxy accelerator (1 wt%) were then added. The samples were formed in stainless-steel molds that had been prepared

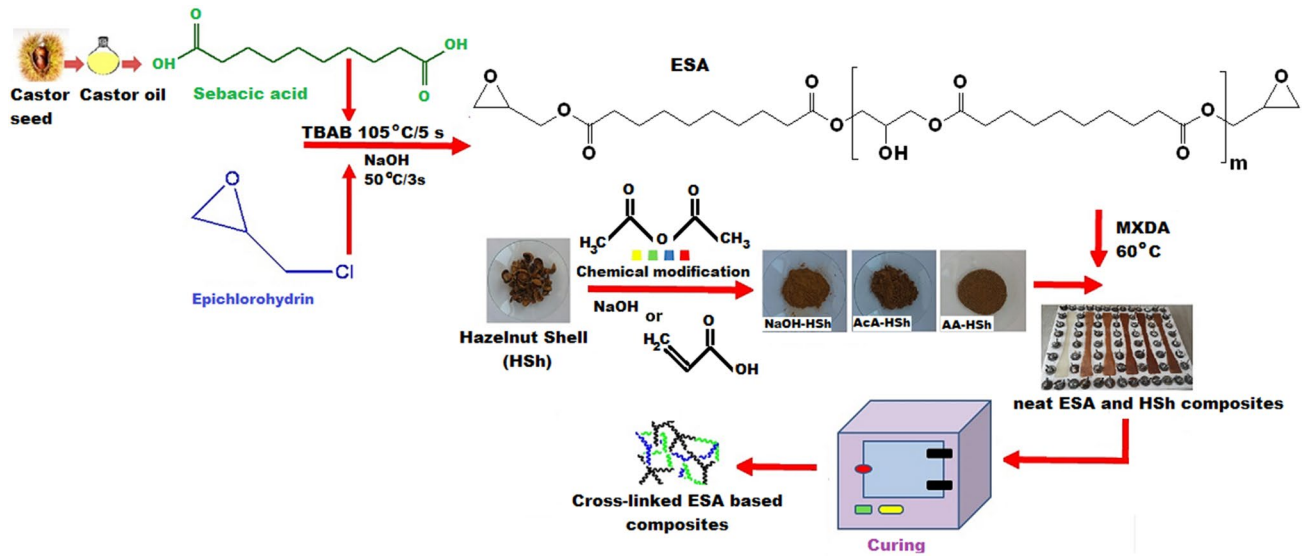

Fig. 1 Schematic showing of ESA synthesis and the preparation of HSh composites

according to the ASTM D 638 standard and cured at 60 ºC (Fig. 1).

Analysis and Measurements

The FTIR spectra of the ESA and HShs were obtained with Bruker-Platinum ATR- vertex 70 (Germany) between 500 and 4000 cm^{-1} wavenumbers at a resolution of 4 cm^{-1} using an attenuated total reflectance (ATR) accessory.

The proton nuclear magnetic resonance (^1H NMR) spectra were obtained using Bruker Ascend 600 magnets at 400.13 MHz and 25 °C (the sample was dissolved in $CDCl_3$).

The scanning electron microscopy (SEM) analyses were performed on a Zeiss EVO LS10 electron microscope with a Bruker 123 eV EDX sensor after the samples were gold-coated by an electro deposition technique to provide electrical conductivity.

Powder X-ray diffraction (XRD) analyses were performed using a Bruker D8 Advance Powder Diffractometer with Cu-K α radiation (λ = 1.5406 A, power = 40 kV). All XRD analyses were performed at room temperature and the scanning was ranged from 10º to 80º.

The thermal analyses were performed with a Mettler Toledo Thermo Gravimetric Analyser. Samples (approx. 10 mg) were heated under a nitrogen atmosphere from 50 to 800 °C at a heating rate of 10 °C·min^{-1} during the analyses.

VST vas determined by CEAST HDT Vicat Analyzer with 50 N loading at a constant heating rate of 50 °C/h according to ASTM D 1525 Standard.

Tensile tests were performed (sample size: 150 mm long × 10 mm wide × 4 mm thick) at room temperature (23 ± 1 °C) using a Stretch and Pressing Equipment TST-Mares/TS-mxe at a rate of 5 mm/min, following the ASTM D 638 standard. Hardness tests were conducted with Shore Durometer TH 210 according to ASTM D 2240 Standard. The hardness value (sample size: 6 mm radius × 6 mm thick) was determined by taking average of five readings on each side of the sample. Five samples of each composite material were tested to obtain reliable values for tensile and hardness tests. The average values of the elongation at break (%), the maximum tensile strength (MPa), Young's modulus (GPa), hardness and corresponding standard deviations were calculated.

Water contact angle measurements were performed at five points on each composite samples at room temperature (23 ± 1 °C) using a contact angle goniometer (Kruss Easy Drop) equipped with an automatic dispenser.

The contents of cellulose and acid-insoluble lignin were determined by the Kurschner–Hoffner method and acid hydrolysis, respectively [26].

A CILAS 1190 laser particle size analyzer was used for the particle characterization of HSh.

Results and Discussion

Characterization of ESA and HShs

Chemical Composition of HShs

The lignin, cellulose and hemicellulose contents determined for all the HSh samples are given in Table 1. The Turkish HSh mainly consists of 51.5% lignin and 38.6% holocellulose [27]. Our results are close to these values.

Table 1 Cellulose and lignin contents of HShs

HSh	Hemicellulose (wt%)	Cellulose (wt%)	Lignin (wt%)
Untreated	21.65	26.86	46.70
NaOH treated	18.48	31.80	41.00
AcA modified	17.60	29.40	33.16
AA modified	13.08	28.08	26.80

Following treatment with alkali, the HSh mass decreased by 15.3 wt%, which indicates partial removal of the lignin, hemicellulose, pectin, and waxy substances from the surface [11]. The cellulose content of HSh before and after alkali treatment was determined to be 26.86% and 31.8%, respectively [28]. The hemicellulose content decreased while cellulose content increased after alkali treatment. This is mainly due to the dissolution of certain hemicelluloses from the surface [29]. The treatments with AA and AcA result in the functionalization of lignocellulosic HSh. The AcA reacts with the cellulosic –OH groups of the HSh to form fiber-OCOOCH=CH_2. However, earlier studies have shown that the bonded acetate was present mainly in lignin and hemicellulose [30]. Acetylation of lignocellulosic material is well known as esterification; moreover, the reaction primarily entails the –OH groups and the modification of fiber-OH to fiber-OCO–CH_3, which causes plasticization and reduces the hydrophilicity of cellulose [31]. Therefore, there is a reduction in the hemicellulose, cellulose and lignin contents (Table 1).

SEM

The fracture surface of the synthesized epoxy resin ESA was examined using SEM and is shown in Fig. 2a. As known from literature, generally the SEM micrographs of the DGEBA-type epoxy resins display regular cracks, indicating a typical brittle fracture surface, which accounts for its poor toughness [32]. In contrast, the SEM micrograph of the ESA displays rare cracked and a relatively rough surface indicating increased ductility of the material [33]. Mustata et al. [34] reported that material with reduced cracks suggests resistance to crack propagation and a good impact strength. Likewise, rougher surfaces signify that crack propagation may become more difficult [35] and combined structure consisting of smooth and rough area makes the cured sample with excellent toughness and strength [36]. But polymers used with rough surfaces can suffer plastic deformation [37]. However, the notable voids and nodules-free fracture surface of the ESA indicate the absence of any plastic deformation [38].

SEM of untreated and chemically modified HShs were shown in Fig. 3a–d. The SEM images clearly show morphological differences arising between the HSh particles as a result of the various chemical modifications. It is clearly seen that by alkali treatment were removed wax and oils covering the surface of the HSh particles (which is marked in Fig. 3a) and irregular-shaped particles with a rough surface were predominant (Fig. 3b) because of removing also lignin and hemicellulose (Table 1) [39, 40]. The chemical modification with AcA and AA similarly caused surface changes resulting in the more rough surfaces (Fig. 3c–d).

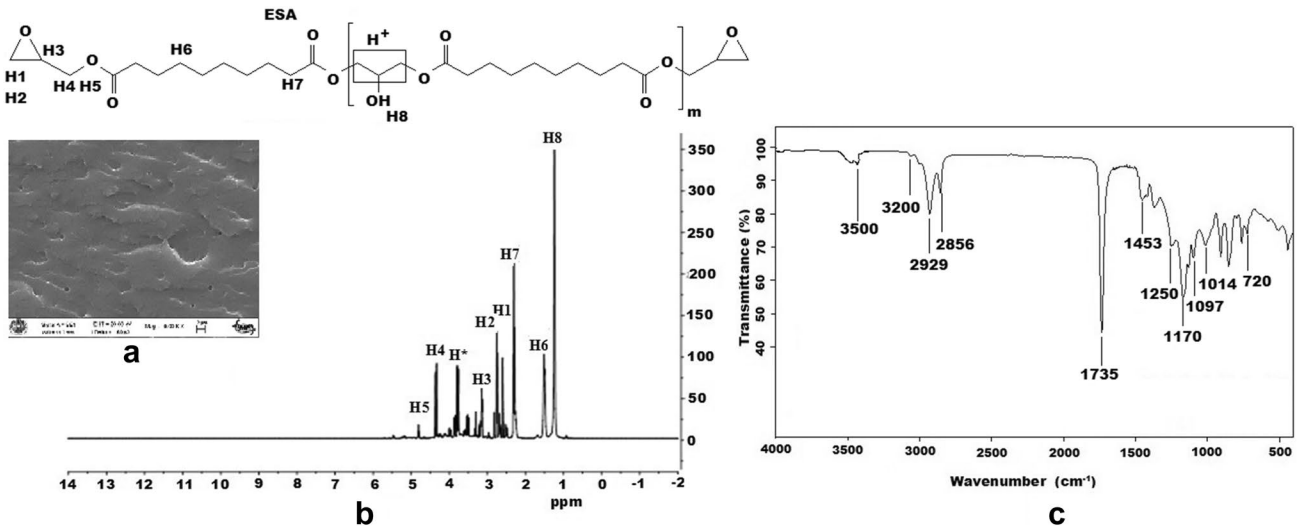

Fig. 2 **a** SEM image; **b** H NMR spectrum; **c** FTIR spectrum of synthesized ESA

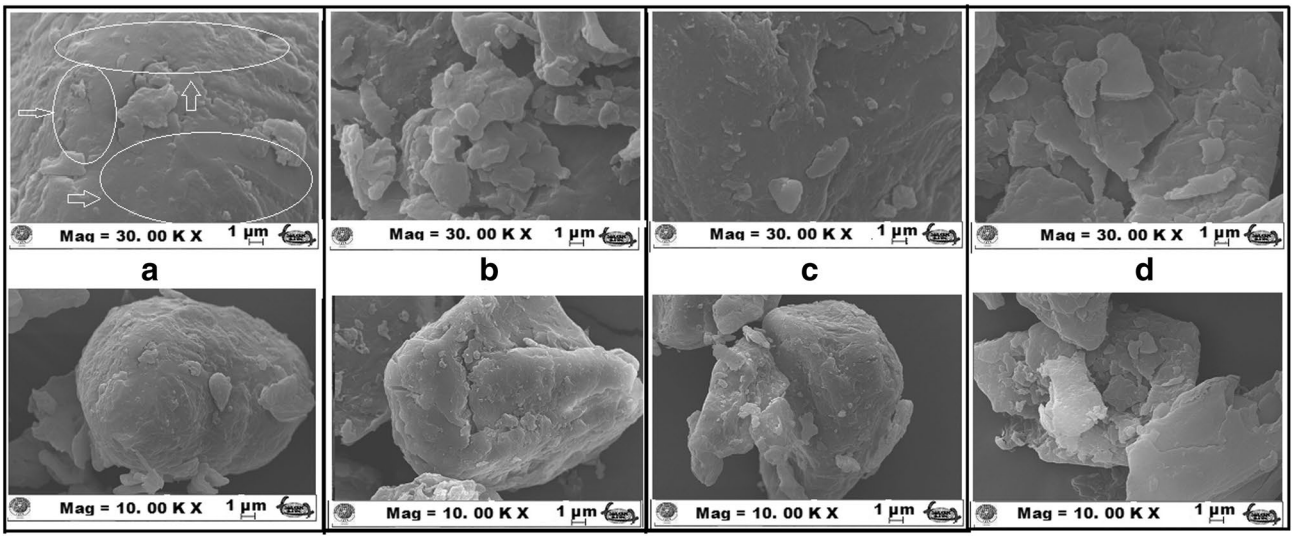

Fig. 3 SEM images of: **a** untreated; **b** alkali treated; **c** AcA modified; **d** AA modified HShs at low and high magnification

^{1}H NMR and FTIR Analysis

The chemical structure of ESA was characterized using the ^{1}H NMR and FTIR spectra (Fig. 2b, c). The ^{1}H NMR spectrum of the ESA (Fig. 2b) indicates the presence of oxygen in the resin structure, and the single peak at δ 1.2 indicates the presence of –OH (H8) in the structure. The single peak at δ 2.3 indicates the presence of the acid –CH_2–C=O group (H7). The –CH_2–CH_2– and R-CH_2-R methylene protons yielded single peaks at δ 1.6 and δ 1.4, respectively (H6). The peak corresponding to –CH_2–OCO– was observed at δ 4.4–4.7 (H4 and H5). The epoxide group was found at δ 2.54–3.2′de (H1, H2 ve H3 protons) [9, 41, 42]. As shown in Fig. 2c, the following peaks were observed in the case of the ESA: the C–H stretching bands of the CH_2 group at 2929 cm^{-1} and 2856 cm^{-1}, and the small characteristic bands of the epoxy and C–Cl groups at 1250 cm^{-1} and 720 cm^{-1}, respectively. Additional bands are observed for the CH_2 group at 1453 cm^{-1}, for the ester C–O bond at 1014 cm^{-1}, for the C–O–C ether stretching at 1170 cm^{-1}, for seconder alcohol at 1097 cm^{-1}, a strong band for the C=O bond at 1735 cm^{-1}, and broad bands for the O–H bond at 3500 cm^{-1} and 3200 cm^{-1} [43].

The FTIR spectra of the untreated and chemically modified HShs are displayed in Fig. 4. As seen in Fig. 4a, the following peaks were observed for the neat HSh: the O–H stretching at 3350 cm^{-1}, the aromatic C=C stretching at 1607 and 1506 cm^{-1}, the stretching of the unconjugated C=O groups present in polysaccharides and xylans at 1737 cm^{-1}, the C–H stretching in –CH_2– and –CH_3 groups at 2917 and 1370 cm^{-1}, and the C–H aromatic ring vibration at 1422 cm^{-1}. The band at 1318 cm^{-1} can be attributed to the presence of syringyl units (C–O stretch), and the peaks at 1028 and 1229 cm^{-1} too can be assigned to the syringyl and guaiacyl (C–O stretch) rings of lignin. The peak at around 895 cm^{-1} in the neat and modified HShs (Fig. 4a-d) is due to the b-glycosidic 1–4 linkage of the glucose ring in cellulose [44]. The intensity of this peak is observed to be higher in all the treated samples than in the untreated HSh, indicating improved cellulose levels. The pH of the solution decreased from 14.2 to 13.49 due to the removal of the carboxylic group by de-esterification [45]. This was further confirmed by chemical analysis. In the FTIR spectrum of NaOH-treated HSh (Fig. 4b), the hemicellulose ketone/aldehyde C=O peak at 1737 cm^{-1} disappeared. The intensity of the C–O stretching of the guaiacyl rings of lignin at 1229 cm^{-1} was lower in the spectra of the treated samples than in that of the untreated HSh, validating a reduction in the quantity of lignin [46]. The AA and AcA treatments of the alkali-treated HSh were further confirmed by FTIR (Fig. 4c, d). The reappearance of the C=O bands at 1739 cm^{-1} in the FTIR spectra following modifications of the alkali-treated HSh confirmed the chemical bonding of AA and AcA. Moreover, the band at 1245 cm^{-1} establishes the presence of the acetate group (Fig. 4c).

XRD and Particle Size Distribution

The XRD curves of neat and modified HShs are shown in Fig. 5. It can be seen from Fig. 5a–d that the diffractogram of all four HShs showed peaks mainly at 2θ values of around 15–16°, 22°, and 35°. The peak at 22° is characteristic of cellulose I [47]. Following alkali treatment, the peak at 12°, which was in the amorphous region, disappeared, while the intensity of the peak at 22° increased due to the removal of amorphous hemicellulose from the HSh surface that

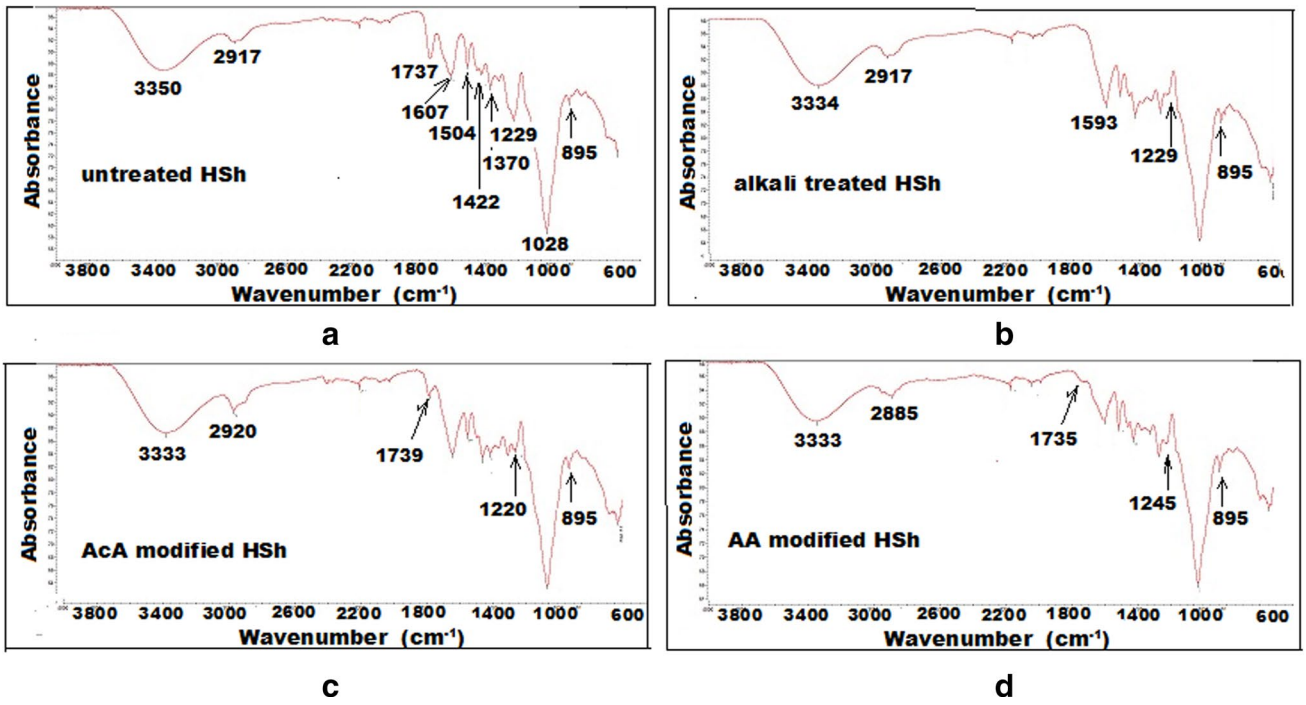

Fig. 4 FTIR spectra of: **a** untreated HSh; **b** alkali treated HSh; **c** AcA modified HSh; **d** AA modified HSh

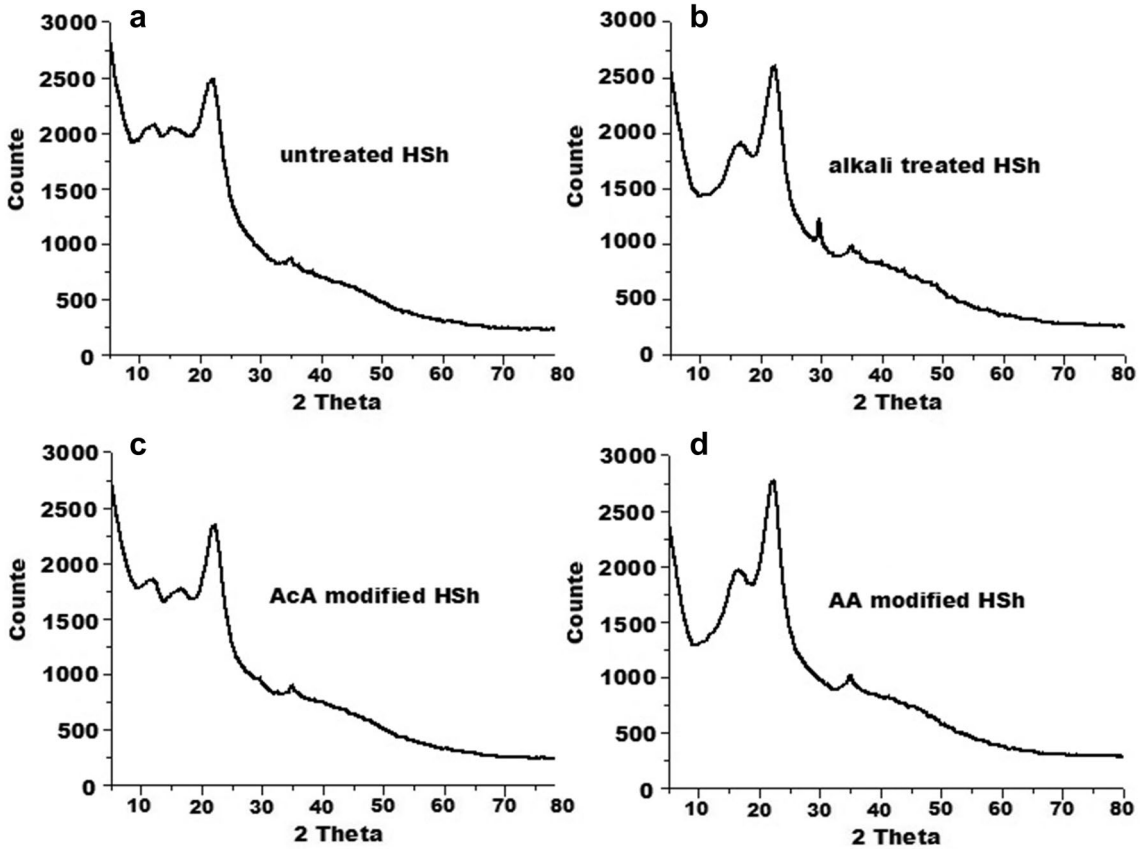

Fig. 5 XRD patterns of: **a** untreated HSh; **b** alkali treated HSh; **c** AcA modified HSh; **d** AA modified HSh

increased its crystallinity [28]. On the contrary, the chemical modification of the HSh particles with AA and AcA resulted in a small decrease in the value of the Segal Crystallinity Index (CrI). The calculated CrI values of the HSh samples is in the order of NaOH-treated (33.33%) > AA-modified (32.72%) > AcA-modified (28.26%) > untreated (24%). The peaks at identical 2θ values, as seen from the XRD patterns of all the samples, indicate that the chemical treatments did not alter the crystalline structure of the HSh [48]. Narendar and Dasan [31] reported analogous information on coir pith treated with different chemicals, and observed that alkali-treated coir pith exhibited higher crystallinity percentage than did the acid-modified samples.

Particle size distribution of untreated and modified HShs and SEM images showing some particle sizes of all HShs are presented in Fig. 6. According to particle size distribution data, the diameter of the particles at 90% distribution of untreated, NaOH-, AcA- and AA-treated HShs were 76.85 ± 2.45 µm, 75.05 ± 1.05 µm, 65.60 ± 0.84 µm and 66.90 ± 0.31 µm, respectively. The SEM images supported the conclusion that most particles were significantly smaller than 106 µm (Fig. 6). As shown in Fig. 6 the diameter of untreated HSh particles decreases after chemical treatments. This small decrease can be associated to the removal of non-cellulosic contents, as well as surface impurities after chemical treatments [49].

Characterization of Composites

SEM

Through SEM study, the effect of filler loading and the bonding between the particles and epoxy matrix in the composites could be determined. Therefore, SEM was used to investigate the morphology of the composites on the cross-section fractures in order to visually evaluate the filler dispersion and the filler–matrix adhesion. In these magnifications, the fillers exiting the matrix plane do not exhibit excellent adhesion between the filler and the matrix [50].

Figure 7 reports fracture surface SEM micrographs of ESA loaded with untreated (Fig. 7a) and chemically modified HShs (Fig. 7b–d). Firstly, the chemical nature of epoxides, polar hydroxyl and ether groups present causes outstanding adhesion to a variety of materials [51]. Especially, it has been observed better wetting of particles with ESA and better filler-matrix adhesion at low HSh loading. Moreover, it is clearly seen that the filler-matrix interaction was improved by chemical treatments. In the untreated HSh composite, it is observed that large particles are dispersed in the ESA. Large particles deform and alter the deformation and failure properties of composites [52]. The number of large particles decreased in order untreated-alkali treated-AcA modified-AA modified HShs. The chemical modification of HSh clearly changed the morphology. The interface adhesion between ESA and modified HSh filler powder in biocomposites showed that the particles did not separate from the matrix. Chemically modified HSh particles with low surface roughness was properly saturated by the ESA, and no visible gap in the interfacial region may suggest good adhesion between the polymer and the filler. In addition to, there is no segregation or filler free part in the fracture surfaces, thus the dispersion of modified HSh particles seems good (Fig. 7b-d) unlike untreated HSh in composite (Fig. 7a).

XRD

The XRD pattern of ESA (Fig. 8a) shows a broad and weak peak centered at $2\theta = 21°$. When a comparison is made

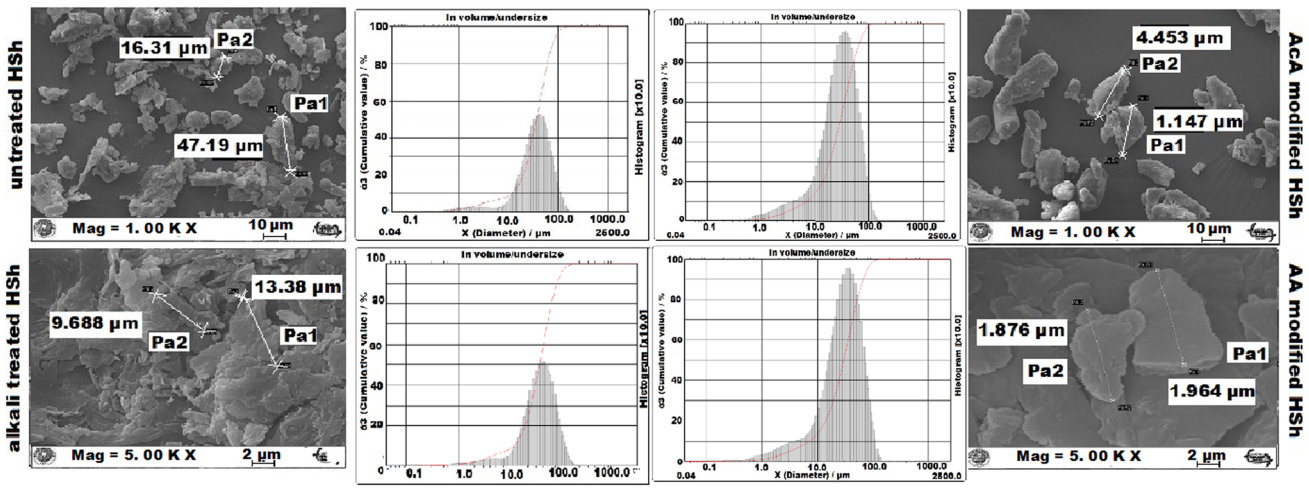

Fig. 6 Particle size distribution of untreated and modified HShs powder with SEM showing a range of particle size and shape belonging to all HShs

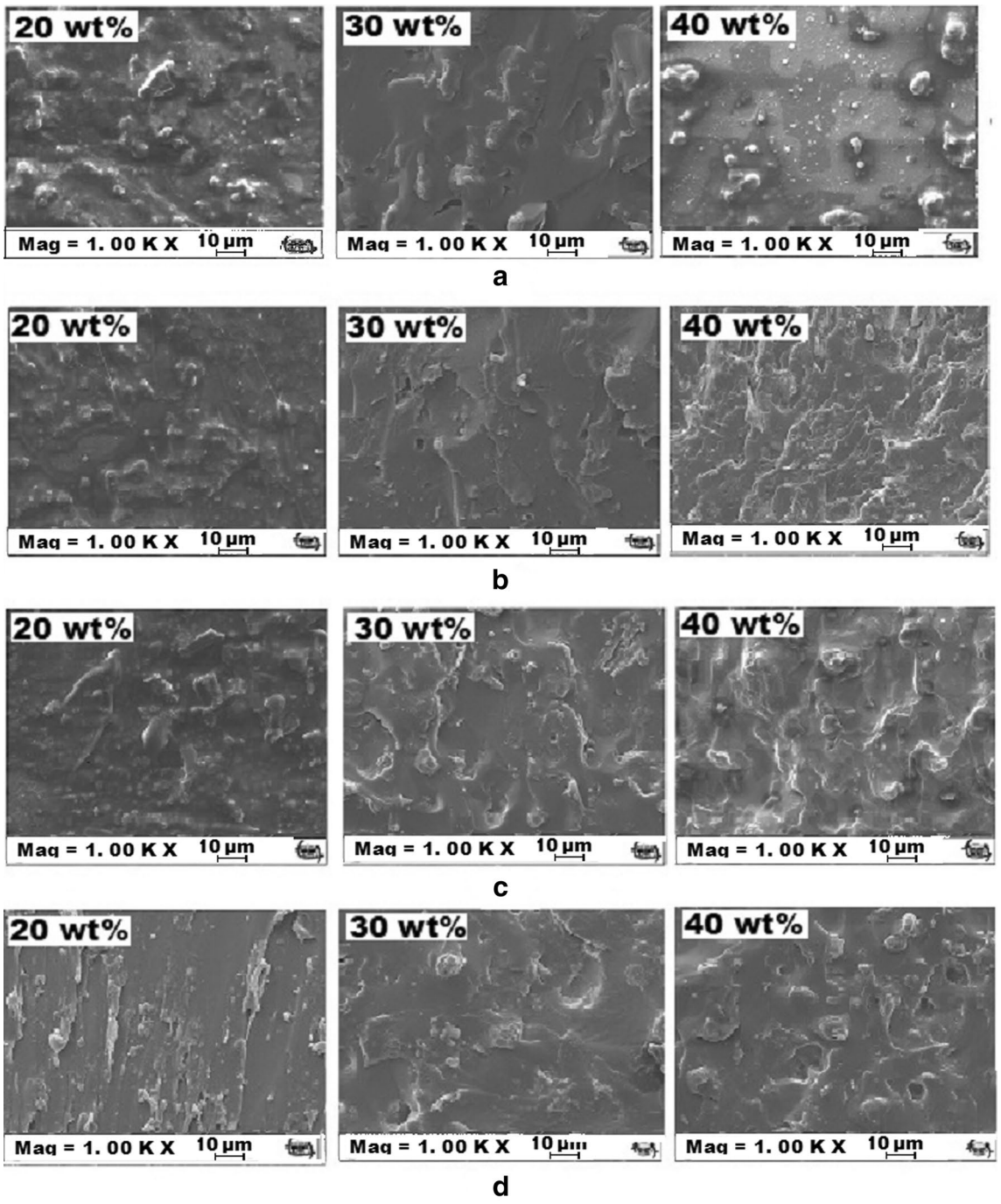

Fig. 7 SEM images of composites with 20–30-40 wt%: **a** untreated HSh; **b** alkali treated HSh; **c** AcA modified HSh; **d** AA modified HSh (Mag.: 1.00 KX; 10 µm)

between the peaks of the neat ESA, HShs (Fig. 5) and composites (Fig. 8a–d), it can be clearly seen that the composites show diffraction patterns similar to those of the matrix. The composites include intensive peaks centered at approximately 22–23° corresponding to the ESA and cellulose I. This provides evidence that the original crystalline structure of the cellulose (cellulose I) is retained in the composites. Additionally, no obvious diffractions are found in composites, and the relatively wide diffraction from 15° to 30° is due to scattering of the cured epoxy molecules, revealing its amorphous nature [53]. This shows that the addition of HShs filler to the epoxy matrix does not lead to significant changes in crystallinity. Thus, the analysis reports that there is no conversion in the transcrystalline phase at the system

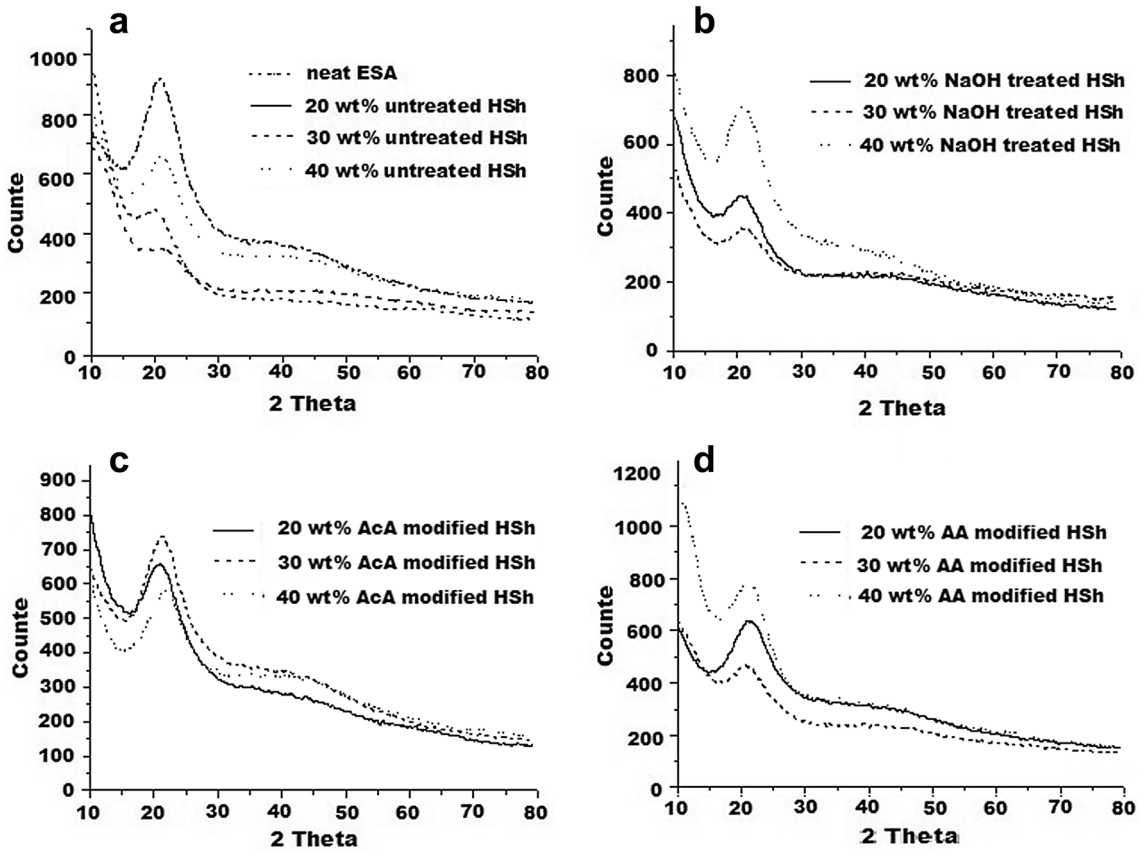

Fig. 8 XRD patterns of composites with 20–30–40 wt%: **a** neat ESA and untreated HSh; **b** alkali treated HSh; **c** AcA modified HSh; **d** AA modified HSh

interface and that there is no change in the 3D cured epoxy network crystal structure induced due to the included HShs filler [54].

Mechanical Properties

The chemical variety of the fillers often leads to differences in particle characteristics. However, the properties of the matrix strongly influence the effect of the filler on the composite properties. The results of the mechanical tests of the composites are given in Table 2. As seen from the values of elongation % at break, tensile strength, Young's modulus and hardness, the various methods of chemical modification affect the mechanical properties differently. The mechanical data determined for ESA are as follows: tensile strength 46 MPa, e-modulus 6.6 GPa, and hardness 84 Shore D. Lignocellulosic fillers in composites exhibit poor compatibility with the polymer matrix and lead to relatively high moisture sorption. Therefore, it is recommended that the fiber surface be modified using various chemical treatments. The removal of fats, lignin, and pectin from the fiber surface by NaOH treatment improves the fiber's adhesive character and results in a rough fiber surface and increases the cellulose content of particles with polar –OH groups [11].

As reported in previous studies, modification of fibers with anhydrides yielded better results than did other treatments since the fibers obtained exhibited the largest effective surface area available for chemical interaction and mechanical clamping with the matrix [55–57]. Thus, the ESA/AA-modified HSh composites had relatively high tensile strength in the range 60–66 MPa. Table 2 shows that the tensile strengths of alkali treated and modified HSh-reinforced composites are all greater than that of pristine epoxy and untreated HSh composites. Especially, tensile strength of composite with 20 wt% AA modified HSh (66 MPa) is increased about 43% as compared with that of neat epoxy (46 MPa). The increments of tensile strengths of alkali treated and modified HSh-reinforced composites were from 13 to 43%.

The tensile strength of the composites decreased in the order of AA-modified HSh > AcA-modified HSh ~ NAOH-treated HSh > untreated HSh. Nevertheless, the tensile strength of all the composites obtained was generally higher, while the e-modulus was lower than that of the neat epoxy matrix ESA.

Table 2 Effect of amount and chemical modification methods of HSh on mechanical properties of biocomposites cured with MXDA

Filler (wt%)	Elongation at break (%)	Tensile strength (MPa)	e-modulus (GPa)	Hardness (Shore D)
Neat ESA				
–	1.4 ± 0.1	46 ± 3.2	6.60 ± 0.52	84 ± 6.8
ESA/untreated HSh composites				
10	1.3 ± 0.2	45 ± 3.1	4.78 ± 0.41	87 ± 6.1
20	1.3 ± 0.1	52 ± 2.7	4.66 ± 0.39	88 ± 6.3
30	1.2 ± 0.1	37 ± 2.8	3.77 ± 0.35	88 ± 6.4
40	1.2 ± 0.3	39 ± 2.9	3.27 ± 0.33	89 ± 6.5
50	1.1 ± 0.3	40 ± 3.2	3.25 ± 0.31	88 ± 6.4
ESA/NaOH treated HSh composites				
10	1.4 ± 0.2	61 ± 4.4	4.25 ± 0.38	86 ± 6.2
20	1.4 ± 0.1	63 ± 4.6	4.68 ± 0.40	87 ± 6.3
30	1.3 ± 0.1	61 ± 4.5	4.18 ± 0.37	88 ± 6.5
40	1.3 ± 0.2	52 ± 3.8	5.20 ± 0.46	86 ± 6.4
50	1.1 ± 0.1	54 ± 3.9	5.23 ± 0.47	86 ± 6.5
ESA/AcA modifed HSh composites				
10	1.8 ± 0.3	60 ± 4.6	4.59 ± 0.38	83 ± 6.0
20	1.9 ± 0.1	65 ± 4.8	4.38 ± 0.34	84 ± 6.2
30	1.9 ± 0.2	59 ± 3.9	4.86 ± 0.43	84 ± 6.3
40	1.7 ± 0.3	57 ± 3.8	4.72 ± 0.40	84 ± 6.3
50	1.6 ± 0.2	50 ± 3.4	3.92 ± 0.39	83 ± 6.2
ESA/AA modifed HSh composites				
10	1.6 ± 0.2	63 ± 4.8	5.12 ± 0.45	85 ± 6.4
20	1.5 ± 0.1	66 ± 4.9	5.66 ± 0.47	85 ± 6.5
30	1.5 ± 0.3	63 ± 4.2	5.25 ± 0.42	85 ± 6.6
40	1.3 ± 0.2	61 ± 4.0	5.20 ± 0.43	83 ± 6.4
50	1.2 ± 0.2	60 ± 4.1	6.72 ± 0.49	84 ± 6.5

The significant reduction of the elongation at break and impact resistance values are typical in the production of polymeric composites with fillers in the form of short fibers or particles [58]. Higher values of Young's modulus values were also observed in the ESA/AA-modified HSh composites. Elongation % at break showed a tendency to decrease with increase in the filler ratio of the composites. However, modifications increased the elongation % of the composites as compared to that of the neat ESA, and greater elongation was observed in the composites prepared with AcA- and AA-modified HShs. The 20 wt% acrylated HSh bio-based epoxy composite showed 44.2% higher tensile properties compared to the untreated HSh composite. Woody HSh is adequately tough because of its high lignin content (approximately 40–51%) [44, 59]. Therefore, composites with untreated HSh had slightly higher hardness values than did neat epoxy. The results of the hardness test revealed that chemically modified HShs did not significantly affect the hardness of the composites when compared with the epoxy. As a result, alkali treatment and chemical modifications were found to be highly suitable for HSh surface modification with respect to improvements in the mechanical properties of the composites.

Other than modification, another factor affecting the mechanical properties of composites are particle size, particle–matrix interface adhesion and particle loading. Particle size has an obvious effect on the mechanical properties and has been investigated by many authors. These studies demonstrated that the tensile strength of composites increases as the size of filler decreases [60–62]. As stated above (Sect. "3.1.4"), particle size of HShs decreased by alkali treatment or chemical modification and as a result the higher tensile strength were determined for modified HShs composites.

Thermal Properties

The TGA curves of neat ESA and composites reinforced with a more appropriate amount (20 wt%) of HSh-based fillers are shown in Fig. 9. Thermal properties including initial decomposition temperature (IDT) at which degradation becomes, T_5, T_{10}, and T_{50} at which 5%, 10% and 50% degradation occur, and residue known as char which is non-volatile part of the composite materials at 800 °C are

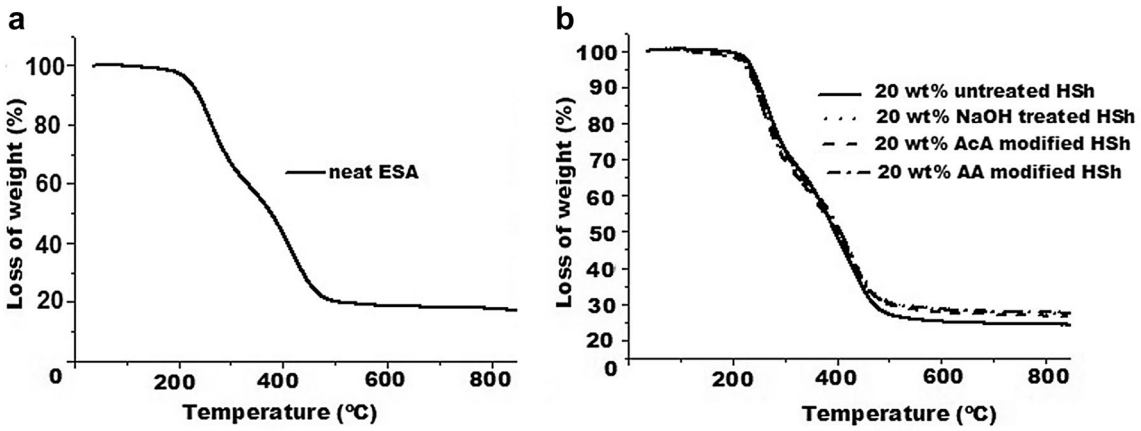

Fig. 9 TGA curves of: **a** neat ESA; **b** composites with 20 wt% HSh filler

given in Table 3. The ~2 % mass loss at around 100 °C is likely caused by moisture. Neat ESA started to decompose at 158 °C. Disregarding the moisture loss, the composites with untreated, NaOH-, AcA- and AA-treated HShs are thermally stable up to 211 °C, 217 °C, 210 °C, and 218 °C, respectively.

The decomposition of hemicellulose starts at approximately 200 °C while that of cellulose and lignin generally begin at 315 °C [63]. Thus, the use of lignocellulosic HSh waste caused an increase in the IDT, T_5, and T_{10} decomposition temperatures of the epoxy matrix although chemical modification of HSh with slightly decreased these values. These results are identical to those previously obtained by us using lignocellulosic coconut waste [11]. When heated to over 600 ºC, the remnants revealed a carbonaceous residue. The residual weight percentages of the composites at 800 °C were in the range 26.7–27%. Due to the very high proportion of lignin in HSh, the % reduction in lignin by alkali treatment did not significantly affect the char amount of the composites.

Vicat softening temperature (VST) is the temperature where flat-ended needle under specified load penetrates the sample to a depth of 1 mm [64]. VST values of ESA and HSh composites with 20 wt% are given in Table 3 and as seen the addition of a HSh filler (20 wt%) produced an increase in VST values. A good rule of thumb is the higher the materials hardness value, the higher its' Vicat softening value will be. The higher hardness values were determined for untreated HSh composites (see Table 2) and in our opinion, accordingly 20 wt% untreated HSh composite has a highest VST value. In Fombuena et al [65] study also was reported that composite with higher Shore D hardness has higher VST value.

Surface Wettability Properties

Surface wettability is one of the most substantial properties for determining the use of a material in a particular application. Determination of wettability is based on the measurement of the material surface contact angle. The wettability depends on surface roughness and chemical composition. Changes of these parameters can adjust the values of contact angle and, therefore, wettability. In the case of pristine polymer materials, their wettability is unsuitable for a wide

Table 3 TGA data of ESA and composites

HSh-based filler (20 wt%)	IDT (°C)	SDT (°C)	T5 (°C)	T10 (°C)	T50 (°C)	Residue (at 800 °C)	VST (°C)
For neat ESA							
–	158	–	218.4	238.2	377.3	17.8	48.0
For composites							
Untreated	211	301	238.2	253.0	396.8	27.0	57.0
NaOH treated	217	308	229.4	244.5	403.2	26.9	52.2
AcA modified	210	300	233.1	246.8	406.3	27.6	53.6
AA modified	218	307	230.2	244.6	399.5	26.7	53.4

IDT initial degradation temperature, *SDT* secondary degradation temperature, *VST* vicat softening temperature, T_5, T_{10} and T_{50} degradation temperatures of 5%, 10%, and 50% weight loss

range of applications (such as tissue engineering, printing, and coating) [66].

The hygroscopicity of the lignocellulosic fillers used in polymers highly correlated with the formation of hydrogen bond between free hydroxyl groups on the fillers and water molecules. Such modifications not only improve their wettability with the polymer matrices, but also reduce the moisture absorption, sometimes impart unique properties and ease of processing. Chemical surface modification methods (acetylation, silane treatment, etc.) the most preferred in this regard [67].

In order to determine how effects the HSh modification on wetting properties of epoxy composite materials, the water contact angle (C.A.) measurements were performed for neat ESA and ESA/50 wt% HShs composites. The images and C.A. values are shown in Fig. 10. Low C.A. values (< 90°) correspond to high wettability and hydrophilic surface, while high values (> 90°) correspond to low wettability and hydrophobic surface. Thus, the C.A. of the materials is higher when the water sorption is lower [68]. The C.A. value of the epoxies is approximately 76° and varies in the range 63–82° for nylons. With the addition of untreated, alkali treated, AcA and AA modified HShs, the contact angle of ESA increased from 84° to 108.5°, 96.8°, 102.4°, and 98.5°, respectively, which indicate that the addition of HShs can be a useful way to improve hydrophobicity of the neat ESA (Fig. 10). The highest C.A. (108.5°) was observed in the case of the untreated HSh composite.

As known, the order of polarity of the functional groups is carboxyl > amide > hydroxyl > ketone, aldehyde > amine > ester > ether > alkene > alkane. Moreover, the polarity of aromatic compounds and conjugated polyenes is higher than that of alkanes and alkenes [69]. The ESA has polar hydroxyl, ester, and epoxy groups, and hence reinforcement with HSh decreased its wettability. It was reported in literature that more hydrophilic filler than matrix increased the hydrophilicity of the materials [70]. The alkali treatment and chemical modification of HSh is seen also affect its wettability. It is reported that the surface roughness of the fibers and accessibility of hydroxyl groups on the surface are the two important factors affecting surface wettability.

Alkali treatment reduced the water contact angle of the lignocellulosic filler, which become more hydrophilic after the NaOH treatment [11] because of treatment of the natural fiber leads to the swelling of the fiber and removal of lignin, resulting in increased moisture absorption. Consequently, the lower C.A. is observed in the alkali treated HSh composite. After, in acetylation treatment acetyl group (–CH_3COO) reacts with the hydrophilic hydroxyl groups of the fibre and takes out the existed moisture. The fibre became more hydrophobic due to the substitution of hydroxyl groups with acetyl groups [67] and therefore, the C.A. of composite increased. The same event occurs with AcA modified HSh composite.

Comparison with Other Biocomposites

The mechanical and thermal results (tensile strength, max. degradation temperature and Vicat softening temperature) determined for the new epoxy composites reinforced with HSh filler material were compared with results pertaining to other alternative composites (Table 4). In the literature, there are several reports on the mechanical and thermal properties of composites with bio-waste nutshell fillers [12, 17, 22, 71–78], but the study with the epoxy matrix is limited and Vicat determination has been made in a few studies. Also, it has been seen that in some of the researches only mechanical

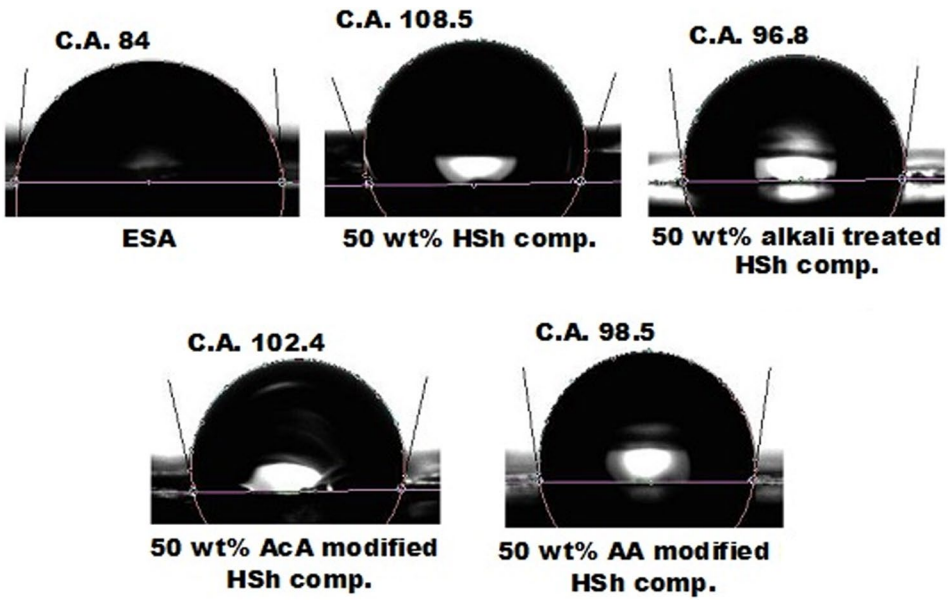

Fig. 10 Water contact angle measurement images of neat ESA and composites with 50 wt% HShs

Table 4 Comparison of the mechanical test and thermal analysis results of biocomposites in present and previous works

Composite	Tensile strength (MPa)	T_{max}* (°C)	VST** (°C)	References
ESA/untreated HSh (20 wt%)	52	500	57.0	This study
ESA/alkali treated HSh (20 wt%)	63	503	52.2	
ESA/AcA modified HSh (20 wt%)	65	510	53.6	
ESA/AA modified HSh (20 wt%)	66	506	53.4	
Epoxy resin/HSh (25 wt%)	30	–	–	[71]
Epoxy resin/alkali treated HSh (40 wt%)	20	–	–	[72]
Epoxy resin/HSh (30 wt%)	43.68	–	–	[73]
Epoxy resin- Acrylated epoxidized soybean oil /HSh (20 wt%)	73	–	–	[74]
PLA/Pekan nutshell (7.5 wt%)	31.4	395	–	[12]
PLA/HSh (20 wt%)	45	365	54.5	[17]
(PLA-7.5–22.5 wt% epoxidized linseed oil)/HSh (20 wt%)	34.4–15.3	370–381	51.5–48.3	
PP/HSh (20 wt%)	27.21	–	159	[22]
HDPE/HSh (30 wt%)	17.2	–	–	[75]
PP/alkali treated Macadamia nutshell (5 wt%)	32.5	–	–	[76]
PP/Argan nutshell (20 wt%)	23	480	–	[77]
PP-SEBS-g-MA/Argan nutshell (20 wt%)	27.5	485	–	
HDPE/alkali treated Argan nutshell (20 wt%)	28.13	453	–	[78]

*T_{max} max. degradation temperature

**VST Vicat softening temperature

properties were examined. As seen from Table 4, the tensile strength, T_{max}. and Vicat values of the ESA composites with 20 wt% HSh loading are varied in the range of 52-66 MPa, 500-510 °C and 52.2-57 °C, respectively. These values reported in the literature varied between 17.2 MPa and 73 MPa, 365 °C and 485 °C, 48.3 °C and 159 °C, respectively generally for 20 wt% filler loadings. Therefore, the HSh-containing ESA-based composites exhibit more favorable results in comparison to the most of the other epoxy or polymer composites. From the Table 4 it is clear that until now no study has been carried on the HSh reinforced bioepoxy composites in order to improve its mechanical, thermal and wettability properties by applying different chemical modifications of filler. These composites are found to have good mechanical and thermal properties.

Conclusion

An alternative to the bisphenol-A type epoxy resin was successfully synthesized using bio-based epoxy with acceptable properties. The other objective of this experimental study was to prepare composites from agricultural waste such as hazelnut shell (HSh). The SEM images clearly show morphological differences arising between the HSh particles as a result of the various chemical modifications. It was found a reduction in the hemicellulose, cellulose and lignin contents after modifications. Alkali treatment and chemical modifications were found to be highly suitable for HSh surface modification with respect to improvements in the mechanical and thermal properties of the composites such as tensile strength, VST, IDT, T_5, and T_{10} decomposition temperatures. The increments of tensile strengths of alkali treated and modified HSh-reinforced composites were from 13 to 43%. The residue (char) values at 800 °C remained higher in the composites with 20 wt% ratios than that of neat ESA. The increasing of contact angle of ESA by addition of untreated and modified HShs indicate that the addition of HShs can be a useful way to improve hydrophobicity of the neat ESA. HSh-containing ESA-based composites exhibit more favorable results in comparison to the most of the other epoxy or polymer composites which suggests its highest applicability as an ecologically-friendly and inexpensive material.

References

1. Battegazzore D, Frache A (2019) J Polym Environ 27:2213
2. Pilla S (2011) Handbook of bioplastics and biocomposites engineering applications. Wiley, New Jersey
3. Miyagawa H, Misra M, Drzal LT, Mohanty AK (2005) J Polym Environ 13:87
4. Sarwono A, Man Z, Bustam MA (2012) J Polym Environ 20:540
5. Niedermann P, Szebényi G, Toldy A (2014) J Polym Environ 22:525
6. Park S-J, Jin F-L, Lee J-R (2004) Macromol Chem Phys 205:2048

7. Thulasiraman V, Rakesh S, Sarojadevi M (2009) Polym Compos 30:49
8. Auvergne R, Caillol S, David G, Boutevin B, Pascault J-P (2014) Chem Rev 114:1082
9. Ma S, Liu X, Jiang Y, Tang Z, Zhang C, Zhu J (2013) Green Chem 15:245
10. Bledzki A, Jaszkiewicz A (2010) Compos Sci Technol 70:1687
11. Kocaman S, Karaman M, Gursoy M, Ahmetli G (2017) Carbohydr Polym 159:48
12. Álvarez-Chávez C, Sánchez-Acosta D, Encinas-Encinas J, Esquer J, Quintana-Owen P, Madera-Santana T (2017) Int J Polym Sci 2017:1
13. Battegazzore D, Noori A, Frache A (2019) J Compos Mater 53:783
14. Demirkaya E, Dal O, Yüksel A (2019) J Supercrit Fluids 150:11
15. Battegazzore D, Alongi J, Frache A (2014) J Polym Environ 22:88
16. Mitra B (2014) Def Sci J 64:244
17. Balart JF, Fombuena V, Fenollar O, Boronat T, Sánchez-Nacher L (2016) Compos B 86:168
18. Balart JF, García-Sanoguera D, Balart R, Boronat T, Sánchez-Nacher L (2018) Polym Compos 9:848
19. Matějka V, Fu Z, Kukutschová J, Qi S, Jiang S, Zhang X, Yun R, Vaculik M, Heliova M, Lu Y (2013) Mater Design 51:847
20. Bryśkiewicz A, Zieleniewska M, Przyjemska K, Chojnacki P, Ryszkowska J (2016) Polym Degrad Stab 132:32
21. Guru M, Aruntas Y, Tuzun FN, Bilici I (2009) Fire Mater 33:413
22. Demirer H, Kartal I, Yıldırım A, Büyükkaya K (2018) Acta Phys Polon A 134:254
23. Müller M, Valášek P, Linda M, Petrásek S (2018) Sci Agric Bohem 49:53
24. Salasinska K, Barczewski M, Borucka M, Górny RL, Kozikowski P, Celiński M, Gajek A (2019) Polymers 11:1234
25. Gu H (2009) Mater Design 30:3931
26. Sluiter A, Hames B, Ruiz R, Scarlata C, Sluiter J, Templeton D, Crocker D (2008) Lab Anal Proced 1617:1
27. Haykiri-Acma H, Yaman S (2007) Fuel 86:373
28. Sonia A, Priya Dasan K (2013) Carbohydr Polym 92:668
29. Obi Reddy K, Uma Maheswari C, Shukla M, Song JI, Varada Rajulu A (2013) Compos B 44:433
30. Prasad PN, Mark JE, Kandil SH, Kafafi ZH (1998) Science and technology of polymers and advanced materials. Springer, New York
31. Narendar R, Priya Dasan K (2014) Compos B 56:770
32. Kocaman S, Ahmetli G (2016) Prog Org Coat 97:53
33. Mandhakini M, Chandramohan A, Rangaraju Vengatesan M, Alagar M (2011) High Perform Polym 23:403
34. Mustata FR, Tudorachi N, Bicu I (2013) Ind Eng Chem Res 52:17099
35. Wang R, Schuman Th, Vuppalapati RR, Chandrashekhara K (2014) Green Chem 16:1871
36. Yang X, Wang Ch, Li Sh, Huang K, Li M, Mao W, Cao Sh, Xia J (2017) RSC Adv 7:238
37. Mellor BG (2006) Surface coatings for protection against wear. CRC Press, Boca Raton
38. Guo X, Xin J, Huang J, Wolcott MP, Zhang J (2019) Polymer 183:121859
39. Melo JDD, Carvalho LFM, Medeiros AM, Souto CRO, Paskocimas CA (2012) Compos B 43:2835
40. Sepe R, Bollino F, Boccarusso L, Caputo F (2018) Compos B 133:217
41. Erdik E (2008) Spectroscopic methods in organic chemistry. Gazi Bookstore, Ankara
42. Wang H, Li FS, Zhu BW, Guo L, Yang Y, Hao R, Wang H, Liu Y, Wang W, Guo X, Chen X (2016) Adv Funct Mater 26:3472
43. Hirose S, Hatakeyama T, Hatakeyama H (2005) Thermochim Acta 431:76
44. Alemdar A, Sain M (2008) Compos Sci Technol 68:557
45. Mwaikambo LY, Ansell MP (2002) J Appl Polym Sci 84:2222
46. Muensri P, Kunanopparat T, Menut P, Siriwattanayotin S (2011) Compos A 42:173
47. Wada M, Sugiyama J, Okano T (1993) J Appl Polym Sci 49:1491
48. Khawas P, Deka SC (2016) Carbohydr Polym 137:608
49. Laaziz SA, Raji M, Hilali E, Essabir H, Rodrigue D, Bouhfid R, El kacem Qaiss A (2017) Int J Biol Macromol 104:30
50. Battegazzore D, Noori A, Frache A (2019) Polym Compos 40:3429
51. Raju GU, Kumarappa S (2011) J Reinf Plast Compos 30:1029
52. Móczó J, Pukánszky B (2008) J Ind Eng Chem 14:535
53. Gong L-X, Zhao L, Tang L-C, Liu H-Y, Mai Y-W (2015) Compos Sci Technol 121:104
54. Saba N, Mohammad F, Pervaiz M, Jawaid M, Alothman OY, Sain M (2017) Int J Biol Macromol 97:190
55. John MJ, Anandjiwala RD (2008) Polym Compos 29:187
56. Kabir MM, Wang H, Lau KT, Cardona F (2012) Compos B 43:2883
57. Zafeiropoulos NE, Dijon GG, Baillie CA (2007) Compos A 38:621
58. Brostow W, Hagg Lobland HE, Khoja S (2015) Mater Lett 159:478
59. Cimino G, Passerini A, Toscano G (2000) Water Res 34:2955
60. Fu S-Y, Feng X-Q, Lauke B, Mai Y-W (2008) Compos B 39:933
61. Kwon S-C, Adachi T, Araki W, Yamaji A (2008) Compos B 39:740
62. Zhang S, Cao XY, Ma YM, Ke YC, Zhang JK, Wang FS (2011) eXPRESS Polym Lett 5:581
63. Liyanage CD, Pieris M (2015) Procedia Chem 16:222
64. Guzel G, Sivrikaya O, Deveci H (2016) Compos B 100:1
65. Fombuena V, Sanchez-Nacher L, Samper MD, Juarez D, Balart R (2013) J Am Oil Chem Soc 90:449
66. Slepickova Kasalkova N, Slepicka P, Kolska Z, Svorcik V (2015) In: Aliofkhazraei M (ed) Wetting and wettability, vol 12. IntechOpen, Moscow
67. Gurunathan T, Mohanty S, Nayak SK (2015) Compos A 77:1
68. Gursoy M, Karaman M (2016) Chem Eng J 284:343
69. Brady JE, Durig T, Shang S (2008) Theories and techniques in the characterization of drug substances and excipients. Academic Press, London
70. Ambone T, Joseph S, Deenadayalan E, Mishra S, Jaisankar S, Saravanan P (2017) J Polym Environ 25:1099
71. Barczewski M, Sałasińska K, Szulc J (2019) Polym Test 75:1
72. Panneerdhass R, Gnanavelbabu A, Rajkumar K (2014) Procedia Eng 97:2042
73. Yovial Y, Marthiana W, Duskiardi D, Habibi H (2017) J Agroind 7:56
74. Kocaman S, Ahmetli G (2017) In: Book of abstracts, Baltic Polymer Symposium, Tallinn, Estonia, p 130
75. Boran S (2016) BioResour 11:1741
76. Cipriano JdeP, Zanini NC, Dantas IR, Mulinari DR (2019) J Renew Mater 7:1047
77. Essabir H, Bensalah MO, Rodrigue D, Bouhfid R, Elkacem Qaiss A (2016) Carbohydr Polym 143:70
78. Essabir H, El Achaby M, EI Moukhtar H, Bouhfid R, El kacem Qaiss A (2015) J Bionic Eng 12:129